scientific reports

Check for updates

OPEN

Modeling current and future distributions of invasive Asteraceae species in Northeast China

Jie Yu[1], Lan Li[1]✉, Hangnan Yu[1], Weihong Zhu[1], Meizhu Hou[1], Jiangtao Yu[2], Meng Yuan[1] & Zhanqiang Yu[1]

The ecological balance and agricultural productivity of northeastern China are seriously threatened by the long-term invasion and spread of Asteraceae plants, which have severely disrupted the region's biodiversity and ecosystem stability. *Ambrosia artemisiifolia* L., *Ambrosia trifida* L., and *Erigeron canadensis* L. are Class 1 malignant invasive species widely distributed across northeastern China. In this context, we selected 36 predictor variables and utilized the MaxEnt model to investigate the influence of current climate on their distribution patterns. Using future climate data, we projected shifts in the distribution dynamics of these three Asteraceae species for two time periods (2041–2060 and 2061–2080) under three climate change scenarios (SSP126, SSP245, and SSP585). The MaxEnt model demonstrated a good predictive impact, with an average area under the curve (AUC) of 0.918. Currently, the three Asteraceae species are primarily found in the southern part of northeastern China. However, due to future climatic changes, their distribution centroids are gradually shifting southwest, leading to an increase in the area of highly suitable zones for these species. Moreover, trend analysis revealed that the potential distribution changes of highly suitable zones for the three Asteraceae species in the southwestern northeastern China are likely to experience an increasing invasive trend under various future climate models. This study provides initial insights into the distribution dynamics of Asteraceae species in northeastern China under climate change, enabling the formulation of plans for managing and preventing the risks and impacts of invasive species.

Keywords Asteraceae, Distribution centroid shifts, MaxEnt model, Invasive species, Future invasion trends

Biological invasions occur when organisms are introduced into new environments, either naturally or through human activities, resulting in economic losses or ecological disruptions that affect biodiversity, agriculture, forestry, livestock, fisheries, and human health[1,2]. In addition to their ecological and economic impacts, some invasive alien plants (IAPs) pose health risks. Studies have shown that their pollen can trigger allergies and asthma[3]. Research has predicted that by 2050, most continents will experience an increase in alien species[4]. China's Ministry of Ecology and Environment published four lists of invasive species between 2003 and 2016, indicating that biological invasions remain a significant global environmental issue in the 21st century.

In China, approximately 75% of invasive plants in the Asteraceae family were intentionally introduced, while 25% spread unintentionally or naturally[5]. Although exotic Asteraceae species contribute to ornamental plant diversity and provide economic and cultural benefits, they also cause significant economic losses in agriculture, forestry, fisheries, and animal husbandry, as well as harming biodiversity and ecosystems. The Chinese government has implemented proactive measures to address the growing threat posed by invasive alien species. On December 20, 2022, the Ministry of Agriculture and Rural Affairs, along with other ministries, released the "List of Key Management Invasive Alien Species" which became effective on January 1, 2023[6]. Three Asteraceae species, *A. artemisiifolia*, *A. trifida*, and *E. canadensis*, are widespread in Northeast China and are classified as Class 1 malignant invasives[7]. *A. artemisiifolia*, originally from North America, was first identified in Hangzhou, China, in 1935. It is highly invasive, affecting agricultural fields and grasslands in over 20 countries, with its pollen causing allergies and severe respiratory issues[8]. *A. trifida*, another native North American species, was discovered in Liaoning in the 1930s. It can harm various crops and cause fatal allergic reactions[9]. *E. canadensis*, discovered in Shandong in 1860, spreads rapidly, damaging crops, inhibiting the growth of nearby plants, and serving as an intermediate host for the cotton bollworm[10].

[1]College of Geography and Ocean Sciences, Yanbian University, Yanji 133002, China. [2]College of Geographical Science, Harbin Normal University, Haerbin 150025, China. ✉email: lilan@ybu.edu.cn

The three Asteraceae species are annual herbaceous plants characterized by high adaptability and invasiveness, with similar environmental requirements for light, soil, and water, and they frequently colonize disturbed habitats such as farmlands, roadsides, and wastelands[11–13]. Given the substantial overlap in their distribution ranges, a joint modeling approach can streamline the analytical process and elucidate their shared environmental responses. Northeastern China hosts a variety of environments with similar ecological conditions that have allowed the rapid spread and extensive proliferation of certain invasive Asteraceae species. The diverse habitats of this region, ranging from agricultural fields to urban edges, provide ideal conditions for these species to establish and thrive, further highlighting the importance of understanding their ecological dynamics through integrated modeling approaches. The rapid economic growth in this region has amplified the number and frequency of invasive species. Among more than 10 significant invasive plants, species such as *Ambrosia trifida* L., *Ambrosia artemisiifolia* L., *Solanum americanum Mill.*, *Solanum carolinense* L., *Erigeron canadensis* L., and *Sicyos angulatus Linn.* are widely distributed and pose serious socioeconomic threats[14]. Thus, analyzing the habitable zones of these invasive species is necessary for predicting and preventing their potential spread.

Predicting the potential geographic distribution of harmful species is essential for assessing the risks posed by them, as it identifies suitable ranges and extents by integrating distributional, biological, and climatic geographic data[15]. The MaxEnt model, which relies on occurrence-only data and has good reliability even with small sample sizes, is one of the many techniques used to simulate species distributions and ecological niches[16]. When selecting environmental variables for the MaxEnt model, the covariance among environmental factors can be quantified using the variance inflation factor (VIF), which serves as a selection criterion[17]. Alternatively, a comprehensive selection can be achieved by combining premodeling, cluster analysis, and Pearson correlation analysis[18]. Both approaches provide reliable results for selecting environmental factors. Moreover, numerous studies have demonstrated the effectiveness of the MaxEnt model in evaluating the potential dispersal of invasive alien plants (IAPs)[19–21].

This study aimed to: (1) identify the potential environmental variables influencing the distribution of Asteraceae in northeastern China; (2) estimate the geographic spread of Asteraceae under various climate change scenarios; and (3) analyze the dispersal trends of Asteraceae across different cities in Northeast China. These results will help determine the current and future suitable habitats for these Asteraceae species, providing a scientific foundation for their management and prevention in northeastern China.

Study area and materials

Study area

Northeastern China, comprising Heilongjiang, Jilin, and Liaoning provinces, along with the eastern part of Inner Mongolia, is a vital economic region characterized by abundant natural resources, a long history of development, and significant economic connections. This region spans 38°40′–53°30′ N and 115°05′–135°02′ E, covering approximately 1.24 million km^2 (Fig. 1). It has a temperate continental monsoon climate with hot summers and annual precipitation ranging from 400 to 1000 mm, primarily occurring during the summer[22]. Densely populated and economically advanced, northeastern China accounted for 7.81% of the country's population in 2020[23,24]. Since the implementation of the Northeast Revitalization Strategy, the region's economic and social development has accelerated, gradually closing the development gap that widened after the reform and opening up, with Gross Domestic Product (GDP) growth rates surpassing the national average[25]. The fertile soils in the

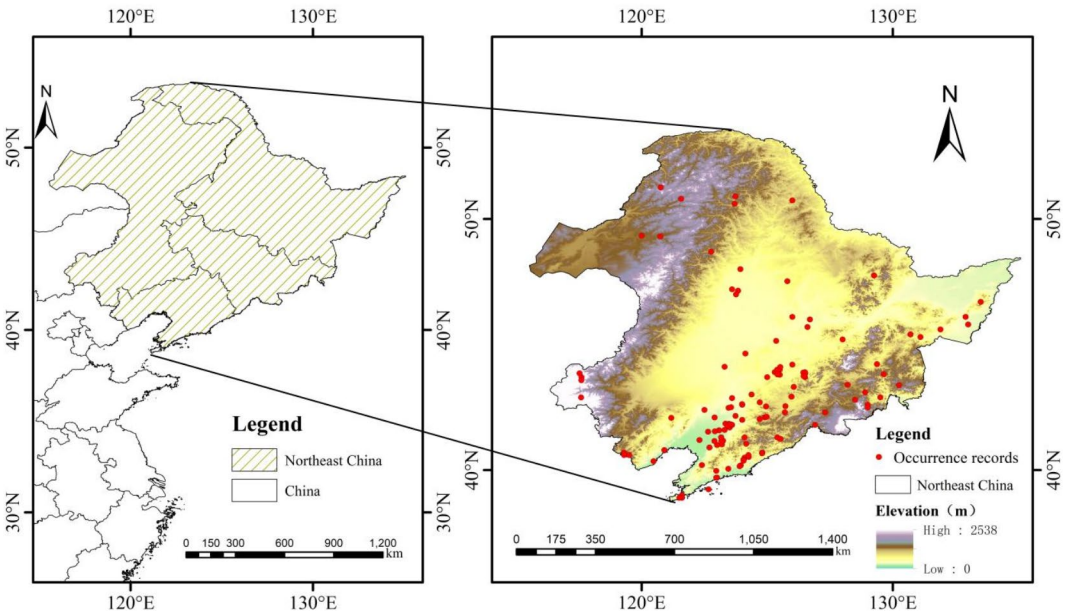

Fig. 1. Location map of the study area and occurrence data for Asteraceae species.

region include black and black-calcium soils in the plains, dark brown forest soils in the mountains, and saline soils in low-lying areas, all of which support abundant agricultural and vegetative resources.

Data on the presence of species and predictive variables

Distribution data for *A. artemisiifolia*, *A. trifida*, and *E. canadensis* were obtained from the Global Biodiversity Information Facility (GBIF;http://data.gbif.org/), the China Virtual Herbarium database (http://www.cvh.ac.cn/), and the China Educational Herbarium Resource Sharing Platform (http://mnh.scu.edu.cn). To prevent model overfitting, we used ENMtools to spatially filter the data points within the study area, removing duplicates and samples lacking detailed coordinates to eliminate positional clustering for model calibration and evaluation[26]. Ultimately, 127 occurrence records were selected for the subsequent analysis of the three Asteraceae species (Fig. 1).

This study selected 36 predictor variables to identify the key factors influencing the distribution of the three Asteraceae species in the northeastern region. Nineteen bioclimatic variables (bio1-bio19) and elevation data (DEM) at 1 km resolution were downloaded from the WorldClim database (https://www.worldclim.org/). Slope (SLO), Aspect (ASP), and Topographic Wetness Index (TWI) were derived from elevation data using ArcGIS Pro (version 3.2). Normalized Difference Vegetation Index (NDVI), Soil pH (SpH), and Soil Moisture (SM) data at 1 km resolution, along with Soil Organic Carbon (SOC) data at 250 m resolution, were obtained from the National Environmental Data Center for the Tibetan Plateau/Third Pole (https://data.tpdc.ac.cn/). Population data (POP) at 1 km resolution were sourced from the Center for International Earth Science Information Network (https://sedac.ciesin.columbia.edu/). Soil type (Soil class), Land Use and Land Cover (LULC), GDP, and Nighttime Light Data (NPP) at 1 km resolution were retrieved from the Resource and Environmental Science Data Registration and Publication System (http://www.resdc.cn/DOI). Roads (RD), Railroads (RR), Waterways (WW), and Built Environments (BE) data were obtained from OpenStreetMap[27] (https://www.openstreetmap.org/) and processed in ArcGIS Pro to calculate Euclidean distances for subsequent analysis with the MaxEnt model. The administrative division data of Northeast China were downloaded from the National Geographic Information Public Service Platform[28] (Tianmap) (https://www.tianditu.gov.cn/).

The 19 bioclimatic variables included present conditions and future projections. Future climate data were derived from the shared socioeconomic pathways (SSPs) outlined in the Intergovernmental Panel on Climate Change (IPCC) Sixth Assessment Report (AR6). To project the potential distribution of Asteraceae, we used the mean outputs of three global circulation models (GCMs): MRI-ESM2-0 (Japan), GISS-E2-1-G (USA), and EC-Earth3-Veg (Sweden). Each GCM was analyzed for two time periods (2041–2060 and 2061–2080) under three climate change scenarios: optimistic (SSP126), moderate (SSP245), and pessimistic (SSP585).

To align with the species distribution data, all predictor variables were resampled to a spatial resolution of 30 arcsec (approximately 1 km). The Spearman correlation coefficient (ρ) was employed in R 4.3.3 to assess correlations among environmental factors. When the correlation between two factors exceeded $|r| < 0.8$, the factor with the highest contribution to the model was retained[9,29] (Table S1, Fig. S1, Fig. S2). We selected eight climatic variables (Table 1), which included two soil, two topographic, and three anthropogenic variables. Table 2 summarizes the forecasting variables prepared in ASCII format for the MaxEnt analysis.

Model configuration and assessment

The potential ranges of the three Asteraceae species were predicted using the MaxEnt model (version 3.4.1). Ten thousand background points were randomly selected as pseudo-absence data. To train the model, 75% of the sample data were randomly chosen, and the remaining 25% were used for testing[30]. The model was built with 10 repetitions of cross-validation, and the average result was taken as the final output. Proper parameter settings were essential for optimizing the model and avoiding overfitting[31]. Regularization multipliers (RM) and feature

Variables	Percent contribution/%	Permutation importance/%
BIO19	29.4	5.6
BIO12	22.9	21.3
LULC	17.3	7.4
RD	7.1	35.1
Soil class	6.5	9.5
POP	2.9	1.7
BIO01	2.7	0.2
BIO11	2.3	1.6
BIO13	1.9	1.9
ASP	1.6	0.9
BIO14	1.3	3.4
SpH	1.3	3.6
BIO09	1.2	2.5
SLO	0.8	2.1
BIO17	0.6	3.3

Table 1. List of predictor variables used in this study and their contribution percentages.

Predictor Variables	Descriptive	Abridge
Climatic variables	Annual Mean Temperature	BIO01
	Mean Diurnal Range	BIO02
	Isothermality (bio02/bio07) (*100)	BIO03
	Temperature Seasonality (standard deviation*100)	BIO04
	Max Temperature of Warmest Month	BIO05
	Min Temperature of Coldest Month	BIO06
	Temperature Annual Range (bio05-bio06)	BIO07
	Mean Temperature of Wettest Quarter	BIO08
	Mean Temperature of Driest Quarter	BIO09
	Mean Temperature of Warmest Quarter	BIO10
	Mean Temperature of Coldest Quarter	BIO11
	Annual Precipitation	BIO12
	Precipitation of Wettest Month	BIO13
	Precipitation of Driest Quarter	BIO14
	Precipitation Seasonality (coefficient of variation)	BIO15
	Precipitation of Wettest Quarter	BIO16
	Precipitation of Driest Quarter	BIO17
	Precipitation of Warmest Quarter	BIO18
	Precipitation of Coldest Quarter	BIO19
Environmental variables	Digital Elevation Model	DEM
	Slope	SLO
	Aspect	ASP
	Topographic Wetness Index	TWI
	Normalized Difference Vegetation Index	NDVI
	Soil type	Soil class
	Soil pH	SpH
	Soil organic carbon	SOC
	Soil Moisture	SM
Anthropogenic variables	Population	POP
	Nighttime Light Data (NPP)	NPP
	Gross Domestic Product	GDP
	Land use and land cover	LULC
	Roads	RD
	Railroads	RR
	Waterways	WW
	Built Environments	BE

Table 2. List of predictor variables used in this study.

combinations (FC) were adjusted, with FC including Linear (L), Quadratic (Q), Product (P), Threshold (T), and Hinge (H)[32,33]. The RM ranged from 0.5 to 4 in intervals of 0.5, and six FC configurations—L, LQ, LQP, LQH, LQHP, and LQHPT—were considered. The R package (version 4.3.3) (ENMevals) was used to select the optimal FC and RM values[34,35], with RM set to 3.5 and FC to LQH for all three Asteraceae species. This combination yielded an optimal model performance, effectively capturing the relationships between environmental variables and species distributions while mitigating the risk of overfitting.

The final 15 variables were used in the MaxEnt model, with the results imported into ArcGIS Pro and converted to raster format. In ArcGIS Pro, the results were reclassified using the natural discontinuity grading method into four habitat suitability categories: Unsuitable, Low suitable, Moderately suitable, and Highly suitable[36]. Model accuracy was assessed using the Receiver Operating Characteristic (ROC) Curve and the area under the curve (AUC) metric. AUC values range from 0.5 to 1.0, where values closer to 1.0 indicate better performance, while a value of 0.5 suggests poor predictive ability[37]. The True Skill Statistic (TSS) is a widely used evaluation method that combines model sensitivity and specificity, effectively addressing biases due to sample imbalance and offering an additional analytical perspective for model assessment[38].

In this research, all analyses were conducted using ArcGIS Pro and R software.

Methods

The shifting centers of distribution of potentially suitable areas for Asteraceae

Habitat migration is a key mechanism and a natural response of invasive alien species to future climate change. By using ArcGIS Pro to add fields for area calculations and conducting spatial analysis to determine the center

of mass, we integrated the MaxEnt simulation results to compare the areas of suitable habitats and the migration of suitability zone centers for Asteraceae species across different time periods and climate change scenarios.

The reference calculation method[39,40] was used to quantify the changes in the zones of High-, Medium-, and Low-suitability, as well as the displacement of their centroids in different periods in the future. These calculations were performed using the following formulas:

$$\begin{cases} x(t) = \sum_{i=1}^{I} \frac{s_i(t) \cdot X_i(t)}{S(t)} \\ y(t) = \sum_{i=1}^{I} \frac{s_i(t) \cdot Y_i(t)}{S(t)} \end{cases} \tag{1}$$

Where t denotes different time periods, I is the number of unit rasters in the suitable zone, $s_i(t)$ is the area of the unit raster at time t, s(t) is the total area of the suitable zone at time t, $X_i(t)$ and $Y_i(t)$ are the center-of-mass coordinates of the unit raster of the suitable zone at time t, and X(t) and Y(t) are the center-of-mass coordinates of the suitable zone at time t.

$$D = \sqrt{(x(t+1) - x(t))^2 + (y(t+1) - y(t))^2} \tag{2}$$

$$\theta = \operatorname{arctg}\left(\frac{y(t+1) - y(t)}{x(t+1) - x(t)}\right) \tag{3}$$

where D is the displacement distance from the center of mass of the suitable zone at time slot t to time slot t + 1, θ is the direction of center-of-mass displacement in the habitable zone from time period t to t + 1, 0° < θ < 90° indicates that the displacement direction is northeast, 90° < θ < 180° indicates that the displacement direction is northwest, 180° < θ < 270° indicates that the displacement direction is southwest, and 270° < θ < 360° indicates that the displacement direction is southeast.

Sen slope estimate test and Mann-Kendall

The Sen slope estimate, also known as the Theil-Sen median technique[41], is a reliable nonparametric method for determining trends. It is particularly effective with long time-series data and is computationally efficient. Additionally, it is insensitive to measurement errors and outliers[42]. The formula is as follows:

$$\beta = Median\left(\frac{x_j - x_i}{j - i}\right), j > i \tag{4}$$

Where Median ( ) represents the median value. If β is greater than zero, it indicates an increasing trend in the Asteraceae suitable area; conversely, if β is less than zero, it signifies a decreasing trend.

A nonparametric technique called the Mann-Kendall (MK) test was used to identify patterns in the time-series data[43]. This method works well with long time-series, is unaffected by missing values and outliers, and does not require a normal distribution of measurements. Trend significance was assessed using the test statistic Z, calculated as follows:

$$S = \sum_{i-1}^{n-1} \sum_{j=i+1}^{n} sign(x_j - x_i) \tag{5}$$

Where sign ( ) is the sign function, calculated as

$$sign(x_j - x_i) = \begin{cases} +1 & x_j - x_i > 0 \\ 0 & x_j - x_i = 0 \\ -1 & x_j - x_i < 0 \end{cases} \tag{6}$$

$$Z = \begin{cases} \frac{S}{\sqrt{Var(S)}} & (S > 0) \\ 0 & (S = 0) \\ \frac{S+1}{\sqrt{Var(S)}} & (S < 0) \end{cases} \tag{7}$$

Where S is the test statistic, Z is the standardized test statistic, n is the length of the dataset, x_j and x_i are the sample time-series data, and n is the number of sequence samples. When $n \geq 8$, S is approximately normally distributed, with variance calculated as:

$$Var(S) = \frac{n(n-1)(2n+5)}{18} \tag{8}$$

Combining the β and |Z| values, the trends were categorized into five classes. Trend significance was evaluated at the 0.05 confidence level (|Z| ≥ 1.96). Five levels of trend shift were identified by combining the results of the trend analysis: Significant increase (β > 0, |Z| ≥ 1.96), slight increase (β > 0, |Z| < 1.96), relatively stable (β = 0, |Z| < 1.96), slight decrease (β < 0, |Z| < 1.96), and significant decrease (β < 0, |Z| ≥ 1.96).

Results

Current spatial distribution of Asteraceae

In this study, model performance was evaluated using the AUC of the ROC curve. With a default RM of 3.5 and an LQH feature combination, the model achieved an AUC of 0.918 (Fig. 2). The percentage contribution of each predictor variable was calculated using the MaxEnt model. Based on these percentages, the main factors affecting the potential ranges of the three Asteraceae species in northeastern China were bioclimatic factors. Key contributors included Precipitation of Coldest Quarter (BIO19), Annual Precipitation (BIO12), Annual Mean Temperature (BIO01), Precipitation of Driest Quarter (BIO17), Precipitation of Wettest Month (BIO13), Mean Temperature of Coldest Quarter (BIO11), Precipitation of Driest Quarter (BIO14), and Mean Temperature of Driest Quarter (BIO09). Additionally, higher contributions from LULC, RD, POP, Soil class, SpH, ASP, and SLO indicated that anthropogenic and topographic factors also influenced Asteraceae distribution. Climatic variables accounted for 62.3% of the variation in distribution, followed by human variables at 27.3%, and environmental variables contributing the least at 10.2% (Table 1).

Figure 3 illustrates the potential distributions of the three Asteraceae species in northeastern China based on the current climatic conditions. The highest-risk areas for potential invasion are located in the southern part of northeastern China, including Dalian, Dandong, northwestern Yingkou, Anshan, Liaoyang, southeastern Shenyang, western Fushun, Tieling, Liaoyuan, northern Tonghua, southeastern Changchun, and northwestern Jilin, among others. The highly suitable area covers 7.37×10^4 km^2, the moderately suitable area covers 17.67×10^4 km^2, and the low suitability area covers 35.58×10^4 km^2.

Future spatial distribution of Asteraceae

As illustrated in Fig. 4, the potentially suitable areas for the three Asteraceae species under the three climate change scenarios over the two time periods showed changes. The southern region of northeastern China remains the most critical potential invasion zone. Under various future climate scenarios, the primary distribution zone expands and becomes more continuous. Overall, as climate change intensifies, the potentially suitable areas (including high, medium, and low) for the three Asteraceae species in northeastern China are projected to increase compared with the current climate. Specifically, low-suitability areas are likely to expand under future climate scenarios. Moderately suitable areas are projected to increase in the 2050s and the 2070s under the single-scenario model of SSP585 but are trending downward overall. High-suitability areas tended to expand under the anticipated climate scenarios. During the 2050s, high-suitability areas continued to grow to 11.84×10^4 km^2 – 12.83×10^4 km^2, respectively (Fig. 4a, b, c). During the 2070s, highly suitable areas continued to grow to 11.9×10^4 km^2 – 12.80×10^4 km^2, respectively (Fig. 4d, e, f). This growth was mainly due to the shift and spread of medium-to-high-suitability zones.

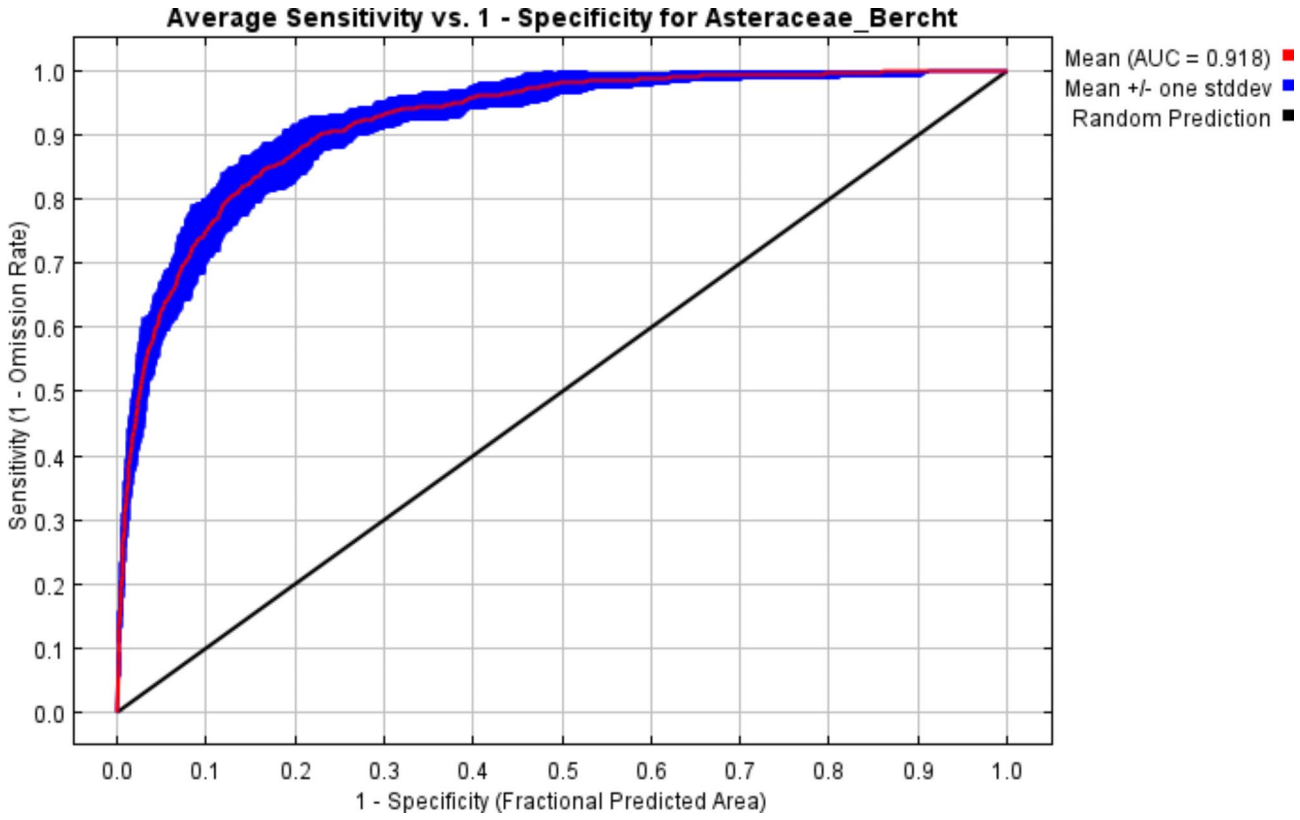

Fig. 2. Predicted ROC curve in the MaxEnt model.

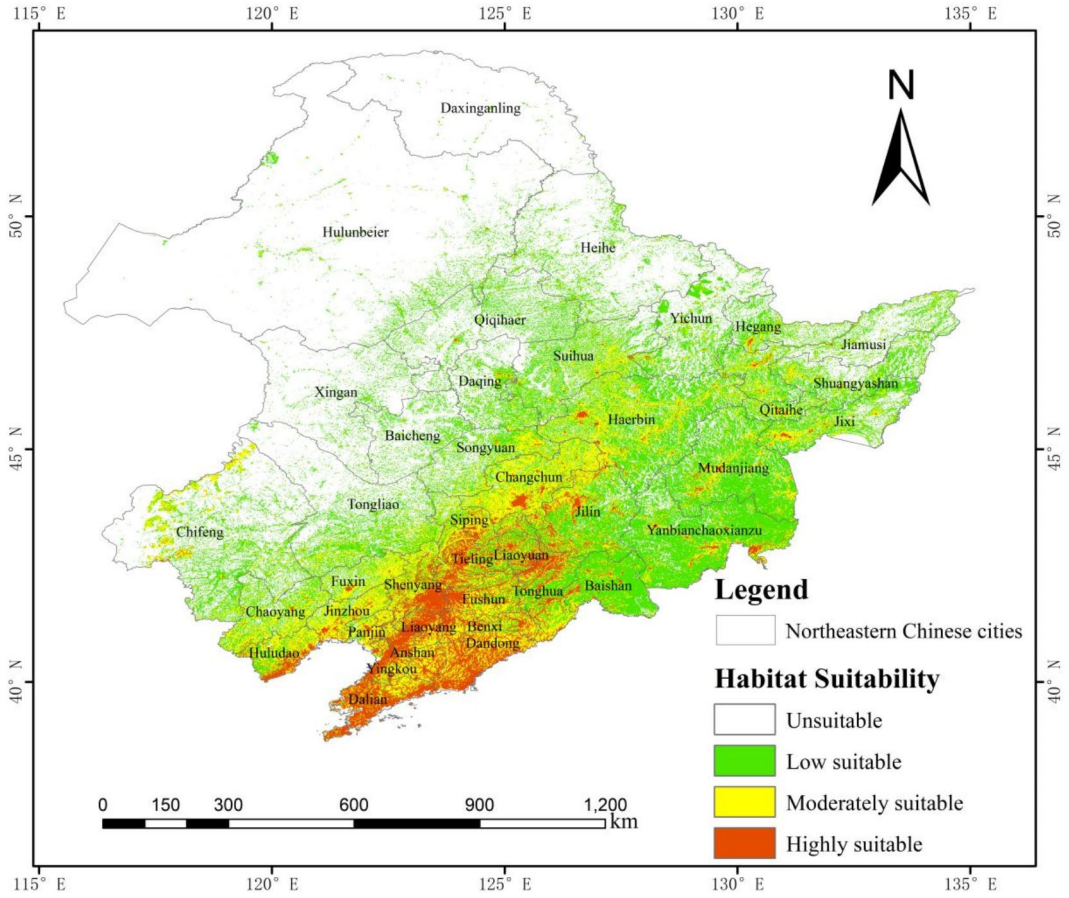

Fig. 3. Potential distribution patterns of the three Asteraceae species based on current climatic conditions.

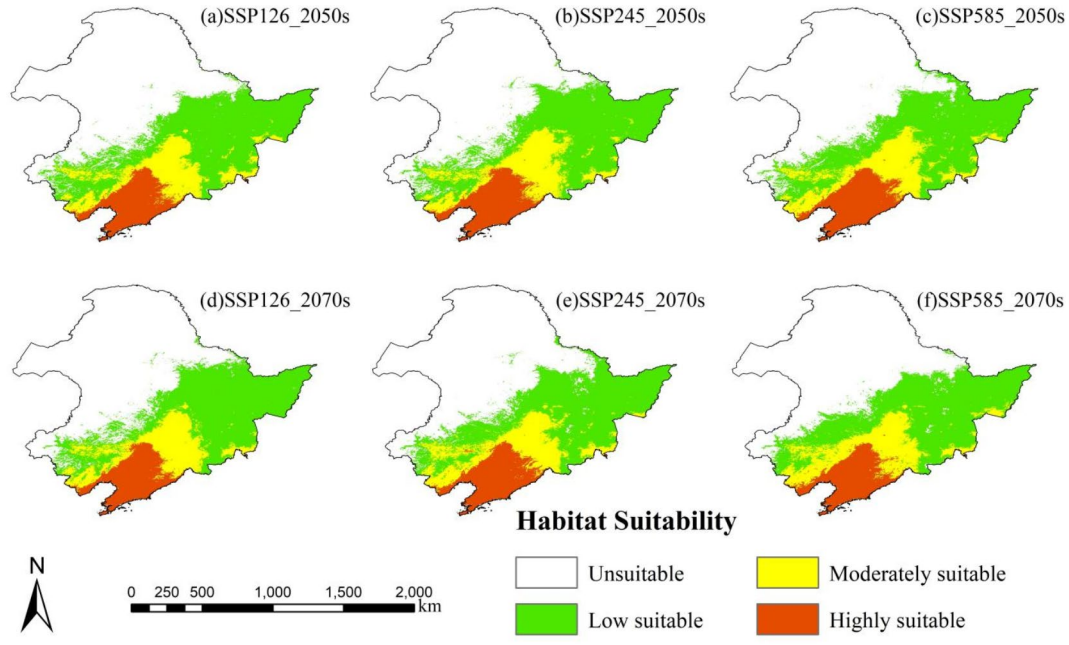

Fig. 4. Potential distribution of three Asteraceae species under different future climate conditions: (**a**), (**b**), and (**c**) are SSP126, SSP245, and SSP585 for the 2050s, respectively. (**d**), (**e**) and (**f**) are SSP126, SSP245, and SSP585 of the 2070s, respectively.

Time	Scenarios	Area ($\times 10^4$ km^2)			
		Expansion	Contraction	Stable	Change
2050s	SSP126	18.32	5.96	54.29	12.36
	SSP245	18.75	5.81	54.44	12.94
	SSP585	19.88	5.83	54.42	14.05
2070s	SSP126	18.32	5.98	54.27	12.34
	SSP245	19.74	5.58	54.67	14.16
	SSP126	19.83	5.89	54.35	13.94

Table 3. Changes in potential habitat area relative to current area for the three Asteraceae species under different climate scenarios.

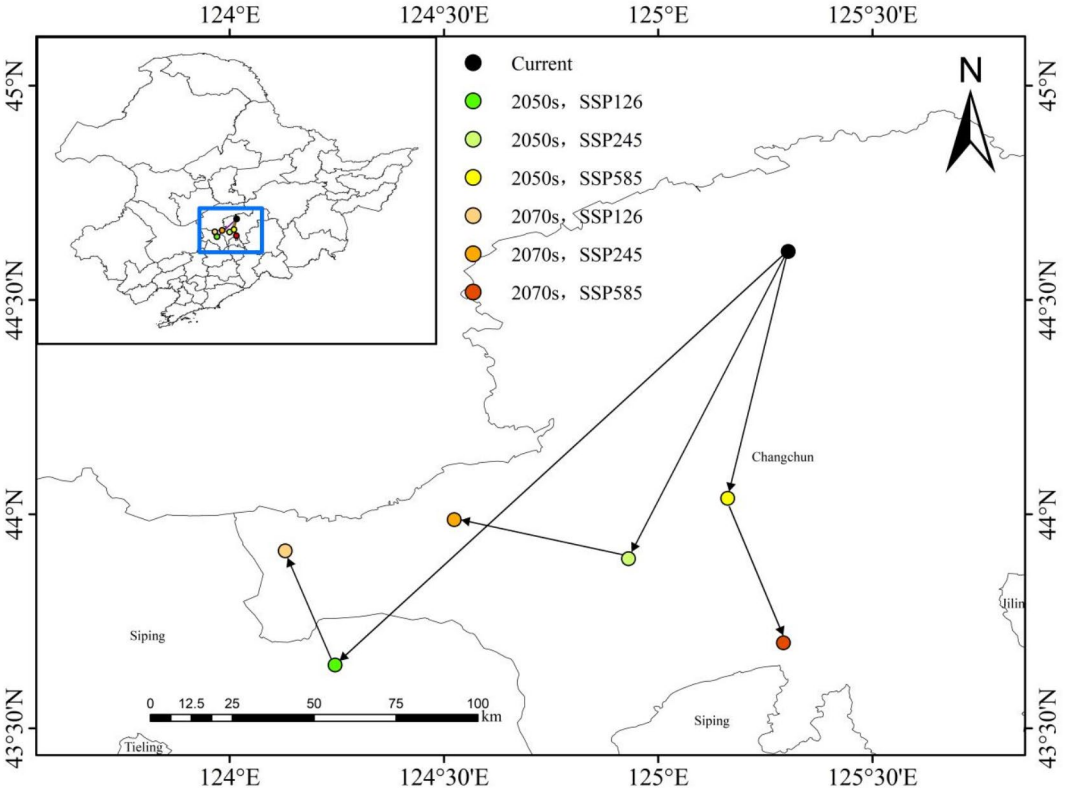

Fig. 5. Centers of mass and their migration in three potentially suitable areas of Asteraceae under different climate change scenarios.

Compared to the current conditions, the suitable areas for the three Asteraceae species in Northeast China are projected to increase (Table 3). In 2050s, the expansion areas under the SSP126, SSP245, and SSP585 climate scenarios were projected to be 18.32×10^4 km^2, 18.75×10^4 km^2, and 19.88×10^4 km^2, respectively. In 2070s, the expansion areas of the habitats of the three Asteraceae species continued to increase, indicating that the species spread more extensively as emission intensity increases. In 2050s, the contraction areas under the three scenarios were 5.96×10^4 km^2, 5.81×10^4 km^2, and 5.83×10^4 km^2, respectively, suggesting that the habitat areas of the three species actually increased by 12.36×10^4 km^2 to 14.05×10^4 km^2. In 2070s, the contraction areas were 5.98×10^4 km^2, 5.58×10^4 km^2, and 5.89×10^4 km^2, respectively, indicating that the habitat areas of the three species increased by 12.34×10^4 km^2, 14.16×10^4 km^2, and 13.94×10^4 km^2, respectively. These findings demonstrate that as emission intensity rises, environmental conditions become increasingly favorable for the invasion of these three Asteraceae species. Among these scenarios, SSP245 in 2070s represents the most favorable conducive for their expansion.

Trends in shifting centers of distribution of potentially suitable areas for Asteraceae

With climate change, the distribution center shifted southwestward (Fig. 5). The current distribution center is located in Nong'an County, Changchun City, Jilin Province (44°36′47″N, 125°18′13″E). Under the SSP126 shared socioeconomic pathway, the distribution center moves 136.596 km southwestward from the current site to Lishu County, Siping City, Jilin Province (43°38′53″N, 124°14′46″E), and then shifts 31.022 km northwestward to

Sen's slope	Z	Trends	SSP126	SSP245	SSP585
≥ 0.0005	≥ 1.96	Significant increase	7.9%	4.3%	7%
≥ 0.0005	−1.96–1.96	Slight increase	5.9%	11.5%	8.3%
−0.0005–0.0005	−1.96–1.96	Relatively stable	31.9%	31.9%	31.9%
< 0.0005	−1.96–1.96	Slight decrease	41.9%	46.7%	49%
< 0.0005	<−1.96	Significant decrease	12.4%	3.7%	3.8%

Table 4. Percentage trends for SSP126, SSP245 and SSP585.

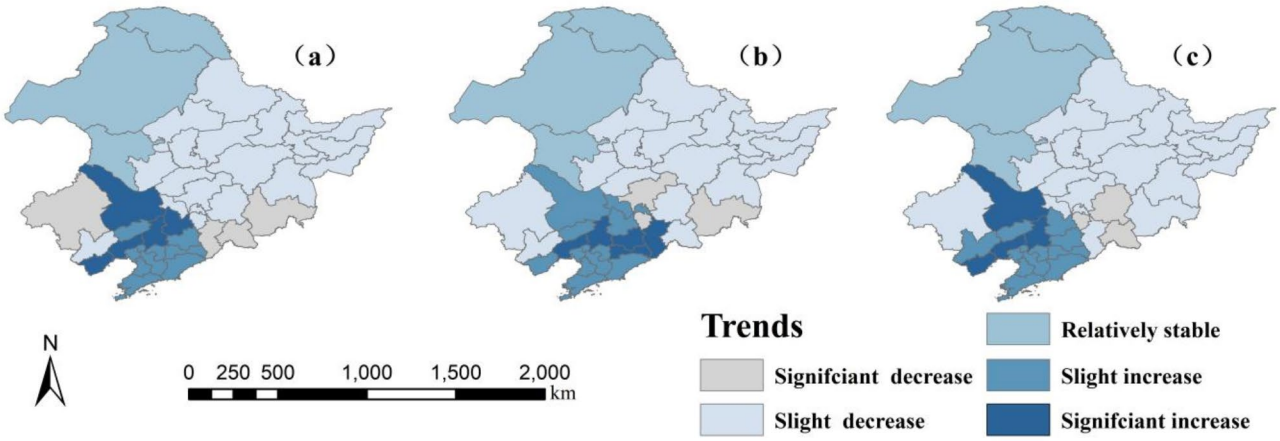

Fig. 6. Trends in the potential distribution of the three Asteraceae species high-suitability zones under different climate models: (**a**) SSP126, (**b**) SSP245, and (**c**) SSP585.

Gongzhuling, Changchun City, Jilin Province (43°54′51″N, 124°7′48″E). Under the SSP245 shared socioeconomic pathway, the distribution center moves 85.047 km southwest from the current site to Gongzhuling, Changchun City, Jilin Province (43°53′46″N, 124°55′51″E), and then moves 34.163 km northwest to Gongzhuling, Changchun City, Jilin Province (43°59′14″N, 124°31′28″E). Under the SSP585 shared socioeconomic pathway, the distribution center moved 64.993 km southwest from the current location to Changchun City, Jilin Province (44°2′13″N, 125°9′44″E), and then moved 38.913 km southeast to Changchun City, Jilin Province (43°41′59″N, 125°17′32″E). Overall, a clear trend of southwestward movement of the distribution centers for these three Asteraceae species was observed, accompanied by an expansion of the primary distribution areas in response to climate change.

Trends in Asteraceae dispersal in different cities under different climate patterns

Sen slope estimation and MK test findings were combined to provide a useful representation of the geographical distribution of future trends in Asteraceae growth across northeastern Chinese cities. The findings were classified into five categories, as shown in Table 4.

In the SSP126 shared socioeconomic pathway, areas of high suitability for the three Asteraceae species in northeastern China significantly increased, primarily in the southwestern cities of Tongliao, Tieling, Shenyang, Jinzhou, and Huludao (Fig. 6a). Regions with both slight and significant increases accounted for 13.8% of the entire region. Under the SSP245 shared socioeconomic pathway, significant increases were observed in Jinzhou City, Shenyang City, Fushun City, Benxi City, and Tonghua City (Fig. 6b), with areas of significant and slight increases accounting for 15.8% of the total area. Under the SSP585 shared socioeconomic pathway, significant increases were mainly observed in Tongliao City, Shenyang City, Jinzhou City, and Huludao City (Fig. 6c), with areas showing both significant and slight increases accounting for 15.3% of the entire region. In summary, Asteraceae species showed an increasing trend in cities in the southern region of northeastern China.

Discussion

Determining the contributions of various factors is crucial for predictive accuracy. Climatic variables best explained the distribution of the three Asteraceae species in northeastern China, followed by anthropogenic factors (Table 1). Originating in North America, these species can easily adapt to similar climatic zones in China near 40°N latitude, enabling rapid population establishment[44]. Among the 15 predictors, the Precipitation of Coldest Quarter (BIO19) was the major factor affecting the distribution of Asteraceae. BIO19 plays a critical role in regulating seed germination and belowground root growth in Asteraceae. While moderate precipitation provides essential moisture for germination, extreme precipitation can result in waterlogged soils, inhibiting germination and promoting root rot[45,46]. Extreme winter precipitation events have dual effects, potentially providing vital moisture while also causing soil erosion and flooding. With global climate change, shifts in

BIO19 trends may alter the distribution range of Asteraceae and threaten the survival of localized populations. Therefore, investigating the dynamics and ecological impacts of BIO19 is essential for understanding the response mechanisms of Asteraceae to climate change. Annual Precipitation (BIO12) and Annual Mean Temperature (BIO01) also significantly affected the distribution, as temperature and precipitation are the primary biological determinants of plant expansion and growth capability[47]. Insufficient precipitation affects the leaves of Asteraceae and limits photosynthesis, with annual precipitation determining whether plants can develop properly during the dry season. Liaoning's average annual temperature from 2020 to 2023 ranged from 9.2 to 10.2 °C, which, along with suitable humidity, supports Asteraceae growth within the 5–15 °C range after dormancy[48–50]. Thus, both mean annual temperature and precipitation significantly affected the distribution of Asteraceae.

Dispersal pathways and reproductive capacity directly affect the spread of Asteraceae. According to previous studies, human activity is closely related to the reproductive ability of Asteraceae[51]. The eight human variables used in this research for prediction include POP, NPP, GDP, LULC, BE, RD, RD, and navigable WW. The findings also demonstrated that LULC, RD, and POP, in addition to climatic factors, affected species distribution (Table 1). With the intensification of human impact, particularly in areas with high population density and increased human activity, the spread and expansion of Asteraceae can be accelerated[45,52]. The findings showed that Soil class and SpH may affect the distribution of Asteraceae, as excessive soil moisture and nutrients enhance their germination and expansion, given that these plants thrive with rapid access to energy[53]. In addition, Asteraceae can grow on various terrains, such as plains, hills, and mountains, owing to their low topographic and soil requirements. Specifically, ASP and SLO are important factors that affect microenvironmental conditions such as light, temperature, and moisture, which, in turn, influence photosynthetic efficiency and growth rate, thereby limiting the dispersal and distribution of Asteraceae[54,55]. Therefore, we can further our understanding of the factors influencing invasive species by measuring the relative significance of environmental and anthropogenic influences.

The southern part of northeastern China, especially Liaoning Province, is a hotspot for Asteraceae invasion (Fig. 3). The three Asteraceae species studied, native to subtropical regions, thrive under favorable hydrothermal conditions due to their light-loving, humidity-loving, heat-tolerant, cold-resistant nature, and high seed production[46]. The climate in southern northeastern China supports their survival, and trade through coastal ports likely contributes to their spread[56]. Many Asteraceae species, such as *Flaveria bidentis (L.) Kuntze* and *Ageratina adenophora*, may have entered China through grain, seed, or horticultural trade[57,58]. The high population density and well-developed transportation in northeastern China facilitated reproduction and spread. As China is the world's largest trading country, more Asteraceae species are continuously introduced through port trade[59,60]. Regulators need to enhance port supervision to mitigate the spread of invasive species, such as chrysanthemums.

Climate change is widely acknowledged to accelerate Asteraceae invasion and expand their global distribution[45,61,62]. In northeastern China, rising temperatures are a result of both climate change and an increase in extreme weather conditions. This study indicated that the major distribution zones of the three Asteraceae species in northeastern China will expand under future climate change (Fig. 4; Table 3). This expansion can be attributed to small seed mass, large seed quantity, rapid maturation, long-lasting seeds, wide climatic tolerance, and high fecundity of the species, which together contribute to a broad geographic range[63,64]. The distribution centroid of Asteraceae was projected to shift southwest (Fig. 5), likely due to increased precipitation in the southwestern part of northeastern China. Since all three species of Asteraceae prefer moist environments and typically thrive in areas with sufficient water availability, their expansion toward the southwest may be attributed to the recent increase in precipitation in this region[65–67]. Consequently, Asteraceae are expected to adjust to climatic alterations and extend their range, supporting the hypothesis that climate change will drive their migration and expansion.

Based on the results of this study, the potential risk of Asteraceae invasion increased in most regions (Fig. 6). Therefore, attention should focus on these areas to enhance control measures and mitigate the impacts of climate change. Current climate conditions and future projections suggest that the distribution center of mass for Asteraceae will mainly reside in Changchun City, Jilin Province. However, the findings suggest that significant movement is unlikely under climate change scenarios. Conversely, under the SSP126 shared socioeconomic pathway, the distribution center of mass for Asteraceae shifts southwestward from Changchun, Jilin Province, to Siping, Jilin Province, indicating greater adaptability to climatic alterations (Fig. 5). Therefore, it is essential to closely monitor the potential expansion of Asteraceae distribution in northeastern China.

While this analysis enhances the understanding of Asteraceae invasive plant distribution and dynamics in northeastern China, there are some limitations. First, the study's limited and unevenly distributed sample points may have overlooked spatial diffusion in areas without samples, implying that the absence of samples does not necessarily indicate no diffusion in those regions. Second, although this study incorporates climatic, environmental, anthropogenic, and socioeconomic factors, it relies on 19 bioclimatic variables for future projections, assuming other factors remain constant. Human contributions are significant, and excluding them may introduce uncertainty; thus, future studies should integrate land-use prediction models to improve accuracy. Additionally, several studies on how climatic changes affect forest species and invasive allergenic plants in Europe have shown that the dispersal capacity of Asteraceae was not sufficiently demonstrated during the relatively short period of introduction[68–71]. This may have contributed to inaccurate findings. Despite these limitations, this study offers predictions of Asteraceae invasion dynamics under climate change scenarios in northeastern China and provides a theoretical foundation for managing these species in the region.

Conclusion

In northeastern China, the MaxEnt algorithm was employed to forecast the potential distribution and dynamic changes of three Asteraceae species, considering the effects of climate, environmental factors, and human

activities. The model showed good performance, as indicated by the AUC values, with the key environmental variables being Precipitation of Coldest Quarter, Annual Precipitation, and Annual Mean Temperature. Under the current climatic conditions, southern northeastern China is a key potential invasion area for Asteraceae, as its climatic conditions are highly suitable for their growth. When combined with ecosystem vulnerability, human activities (such as land use and transportation), and climate change impacts, this region offers ideal conditions for Asteraceae invasion. Future projections estimate that the habitat area of the three Asteraceae species will grow by 12.36×10^4 km^2 to 14.05×10^4 km^2 in the 2050s and by 12.34×10^4 km^2 to 14.16×10^4 km^2 in the 2070s, with distribution centers shifting southwestward. These shifts reflect the species' adaptation to climate change and their range expansion. *A. artemisiifolia* and *A. trifida* are major allergens that cause autumn pollen allergies and pose threats to wheat, barley, and horticultural crops. Meanwhile, *E. canadensis* suppresses the growth of neighboring plants through allelopathy, severely affecting autumn crops, orchards, and tea gardens. These findings aid in understanding the distribution patterns and dynamic changes of the three Asteraceae species under climate change and provide insights for biodiversity protection and oversight in northeastern China. However, owing to the exclusion of human and socioeconomic factors, coupled with the limited and uneven spatial distribution of the data samples, the prediction accuracy may be affected. Future research should incorporate human and economic prediction models to enhance reliability and provide more effective management strategies for ecological managers.

Data availability

All data generated or analysed during this study are included in this published article (and its Supplementary Information files).

Received: 27 August 2024; Accepted: 4 March 2025
Published online: 11 March 2025

References

1. Valéry, L., Fritz, H., Lefeuvre, J.-C. & Simberloff, D. In search of a real definition of the biological invasion phenomenon itself. *Biol. Invasions* **10**, 1345–1351 (2008).
2. Turbelin, A. J. et al. Biological invasions are as costly as natural hazards. *Perspect. Ecol. Conserv.* **21**, 143–150 (2023).
3. Plaza, P. I., Speziale, K. L. & Lambertucci, S. A. Rubbish dumps as invasive plant epicentres. *Biol. Invasions* **20**, 2277–2283. https://doi.org/10.1007/s10530-018-1708-1 (2018).
4. Seebens, H. et al. Projecting the continental accumulation of alien species through to 2050. *Glob. Change Biol.* **27**, 970–982. https://doi.org/10.1111/gcb.15333 (2020).
5. Hao, Q. & Ma, J.-S. Invasive alien plants in China: An update. *Plant Divers.* **45**, 117 (2023).
6. Ministry of Agriculture and Rural Affairs, Ministry of Natural Resources, Ministry of Ecology and Environment, Ministry of Housing and Urban-Rural Development, General Administration of Customs, State Forestry and Grassland Administration Announcement No. 567. Bulletin of the Ministry of Agriculture and Rural Affairs of the People's Republic of China. (12), 53–55 (2022). (in Chinese)
7. China Invasive Species Information System Invasion List (https://www.plantplus.cn/ias/splist) Accessed 13 November 2023.
8. Brandes, D. & Nitzsche, J. Biology, introduction, dispersal, and distribution of common ragweed (Ambrosia artemisiifolia L.) with special regard to Germany. *Nachrichtenblatt-Deutschen Pflanzenschutzdienstes Braunschweig* **58**, 286 (2006).
9. Chen, S., Bai, X., Ye, J., Chen, W. & Xu, G. Prediction of suitable habitat of alien invasive plant Ambrosia trifida in Northeast China under various climatic scenarios. *Diversity* **16**, 322 (2024).
10. Yan, H. et al. Predicting the potential distribution of an invasive species, Erigeron canadensis L., in China with a maximum entropy model. *Glob. Ecol. Conserv.* **21**, e00822 (2020).
11. Dong, H. et al. Causes of differences in the distribution of the invasive plants Ambrosia artemisiifolia and Ambrosia trifida in the Yili Valley, China. *Ecol. Evol.* **10**, 13122–13133 (2020).
12. Kato-Noguchi, H. & Kato, M. Invasive characteristics and impacts of Ambrosia trifida. *Agronomy* **14**, 2868 (2024).
13. Tu, W., Xiong, Q., Qiu, X. & Zhang, Y. Dynamics of invasive alien plant species in China under climate change scenarios. *Ecol. Indic.* **129**, 107919 (2021).
14. Feng, Y. L. *Invasive Plants in Northeast China* (Science Press, 2020).
15. McMahon, D. E., Urza, A. K., Brown, J. L., Phelan, C. & Chambers, J. C. Modelling species distributions and environmental suitability highlights risk of plant invasions in western United States. *Divers. Distrib.* **27**, 710–728 (2021).
16. Merow, C., Smith, M. J. & Silander, J. A. Jr. A practical guide to MaxEnt for modeling species' distributions: What it does, and why inputs and settings matter. *Ecography* **36**, 1058–1069 (2013).
17. Vincent, H. et al. Modeling of crop wild relative species identifies areas globally for in situ conservation. *Commun. Biol.* **2**, 1–8 (2019).
18. Wang, J. et al. Prediction of the future evolution trends of Prunus sibirica in China based on the key climate factors using MaxEnt modeling. *Biology* **13**, 973 (2024).
19. Wan, J. Z., Wang, C. J., Tan, J. F. & Yu, F. H. Climatic niche divergence and habitat suitability of eight alien invasive weeds in China under climate change. *Ecol. Evol.* **7**, 1541–1552 (2017).
20. Guerra-Coss, F. A. et al. Modelling and validation of the spatial distribution of suitable habitats for the recruitment of invasive plants on climate change scenarios: An approach from the regeneration niche. *Sci. Total Environ.* **777**, 146007 (2021).
21. Zachariah Atwater, D. & Barney, J. N. Climatic niche shifts in 815 introduced plant species affect their predicted distributions. *Glob. Ecol. Biogeogr.* **30**, 1671–1684 (2021).
22. Zhang, L. et al. Assessing the remotely sensed evaporative drought index for drought monitoring over Northeast China. *Remote Sens.* **11**, 1960 (2019).
23. Seventh National Census Bulletin (No. 3). National Statistical Office (2021). (in Chinese)
24. Bulletin of the Seventh National Population Census of Inner Mongolia Autonomous Region (No. 1). Statistics Bureau of Inner Mongolia Autonomous Region (2021). (in Chinese)
25. Ren, W., Xue, B., Yang, J. & Lu, C. Effects of the Northeast China revitalization strategy on regional economic growth and social development. *Chin. Geogr. Sci.* **30**, 791–809 (2020).
26. Anderson, R. P. & Gonzalez, I. Jr. Species-specific tuning increases robustness to sampling bias in models of species distributions: an implementation with Maxent. *Ecol. Modell.* **222**, 2796–2811 (2011).
27. Geofabrik GmbH. (2023). OpenStreetMap data extracts for China. Retrieved from https://download.geofabrik.de/asia/china.html

28. National Geographic Information Public Service Platform (Tianmap) (2024). https://cloudcenter.tianditu.gov.cn/administrativeDivision
29. Yang, X.-Q., Kushwaha, S., Saran, S., Xu, J. & Roy, P. Maxent modeling for predicting the potential distribution of medicinal plant, Justicia adhatoda L. Lesser Himalayan foothills. *Ecol. Eng.* **51**, 83–87 (2013).
30. Guo, Y., Wei, H., Lu, C., Gao, B. & Gu, W. Predictions of potential geographical distribution and quality of Schisandra sphenanthera under climate change. *PeerJ* **4**, e2554 (2016).
31. Zhao, Z., Xiao, N., Liu, G. & Li, J. Prediction of the potential geographical distribution of five species of Scutiger in the south of Hengduan Mountains Biodiversity Conservation Priority Zone. *Acta Ecol. Sin* **42**, 2636–2647 (2022).
32. Muscarella, R. et al. An R package for conducting spatially independent evaluations and estimating optimal model complexity for MAXENT ecological niche models. **5** 1198–1205 (2014).
33. Lu, Y. et al. The potential global distribution of the white peach scale pseudaulacaspis pentagona (Targioni tozzetti) under climate change. *Forests* **11**, 192 (2020).
34. Warren, D. L. & Seifert, S. N. Ecological niche modeling in Maxent: the importance of model complexity and the performance of model selection criteria. *Ecol. Appl.* **21**, 335–342 (2011).
35. Ye, X. et al. Prediction of potential suitable distribution of Phoebe bournei based on MaxEnt optimization model. *Acta Ecol. Sin* **41**, 8135–8144 (2021).
36. Wang, X. et al. Habitat suitability assessment of ebdangered plant Alsophila spinulosa in Chishui River area based on GIS and Maxent model. *Acta Ecol. Sinica* **41**, 6123–6133 (2021).
37. Phillips, S. J., Anderson, R. P. & Schapire, R. E. Maximum entropy modeling of species geographic distributions. *Ecol. Modell.* **190**, 231–259 (2006).
38. Allouche, O., Tsoar, A. & Kadmon, R. Assessing the accuracy of species distribution models: Prevalence, kappa and the true skill statistic (TSS). *J. Appl. Ecol.* **43**, 1223–1232 (2006).
39. Hart, J. F. Central tendency in areal distributions. *Econ. Geogr.* **30**, 48–59 (1954).
40. Yue, T.-X., Fan, Z.-M., Chen, C.-F., Sun, X.-F. & Li, B.-L. Surface modelling of global terrestrial ecosystems under three climate change scenarios. *Ecol. Modell.* **222**, 2342–2361 (2011).
41. Ali, R., Kuriqi, A., Abubaker, S. & Kisi, O. Long-term trends and seasonality detection of the observed flow in Yangtze River using Mann-Kendall and Sen's innovative trend method. *Water* **11**, 1855 (2019).
42. Cai, B. & Yu, R. Advance and evaluation in the long time series vegetation trends research based on remote sensing. *J. Remote Sens* **13**, 1170–1186 (2009).
43. Yuan, L. et al. The spatio-temporal variations of vegetation cover in the Yellow River Basin from 2000 to 2010. *Acta Ecol. Sin* **33**, 7798–7806 (2013).
44. Pacanoski, Z. Current situation with invasive Erigeron annuus (l.) Pers. (daisy fleabane) in the Republic of Macedonia. *EPPO Bull.* **47**, 118–124 (2017).
45. Fang, Y. et al. Predicting the invasive trend of exotic plants in China based on the ensemble model under climate change: A case for three invasive plants of Asteraceae. *Sci. Total Environ.* **756**, 143841 (2021).
46. Yang, W. et al. Dynamics of the distribution of invasive alien plants (Asteraceae) in China under climate change. *Sci. Total Environ.* **903**, 166260 (2023).
47. Liu, Y. et al. MaxEnt modelling for predicting the potential distribution of a near threatened rosewood species (Dalbergia cultrata Graham ex Benth). *Ecol. Eng.* **141**, 105612 (2019).
48. Abul-Fatih, H. & Bazzaz, F. The biology of Ambrosia trifida L. II. Germination, emergence, growth and survival. *New phytol.* **83**, 817–827 (1979).
49. Regehr, D. & Bazzaz, F. The population dynamics of Erigeron canadensis, a successional winter annual. *J. Ecol.* **67**, 923–933 (1979).
50. Baskin, J. M. & Baskin, C. C. Ecophysiology of secondary dormancy in seeds of Ambrosia artemisiifolia. *Ecology* **61**, 475–480 (1980).
51. Pyšek, P. et al. Disentangling the role of environmental and human pressures on biological invasions across Europe. *Proc. Natl. Acad. Sci.* **107**, 12157–12162 (2010).
52. Sang, W., Feng, J. & Xue, D. Human, ethnical and social insights of biological invasion. *Chin. J. Cent. Univ. Natl.(Nat. Sci. Ed.)* **17**, 17–23 (2008).
53. Theoharides, K. A. & Dukes, J. S. Plant invasion across space and time: factors affecting nonindigenous species success during four stages of invasion. New phytol. **176** (2007).
54. Zhao, W. et al. Rapid monitoring of Ambrosia artemisiifolia in semi-arid regions based on ecological convergence and phylogenetic relationships. *Front. Ecol. Evol.* **10**, 926990 (2022).
55. Chen, J., Ma, F., Zhang, Y., Wang, C. & Xu, H. Spatial distribution patterns of invasive alien species in China. *Glob. Ecol. Conserv.* **26**, e01432 (2021).
56. Seebens, H. et al. Global trade will accelerate plant invasions in emerging economies under climate change. *Global Change Biol.* **21**, 4128–4140 (2015).
57. Xian-Ming, G. et al. An alert regarding biological invasion by a new exotic plant, Flaveria bidentis, and strategies for its control. *Biodiversity Sci.* **12**, 274 (2004).
58. Axmacher, J. C. & Sang, W. Plant invasions in China–challenges and chances. *PloS one* **8**, e64173 (2013).
59. Wu, S. H., Hsieh, C. F., Chaw, S. M. & Rejmánek, M. Plant invasions in Taiwan: Insights from the flora of casual and naturalized alien species. *Divers. Distrib.* **10**, 349–362 (2004).
60. Huang, Y. et al. Impacts of climate change on climatically suitable regions of two invasive Erigeron weeds in China. *Front. Plant Sci.* **14**, 1238656 (2023).
61. Kueffer, C. Plant invasions in the Anthropocene. *Science* **358**, 724–725 (2017).
62. Xian, X. et al. Climate change has increased the global threats posed by three ragweeds (Ambrosia L.) in the Anthropocene. *Sci Total Environ.* **859**, 160252 (2023).
63. Jian-Hua, H., Sheng, Q., Kang-Ning, D. & Yuan-Xing, G. Wind-dispersed traits of cypselas in ten Asteraceae alien invasive species. *Chin. J. Plant Ecol.* **34**, 957 (2010).
64. Rejmanek, M. & Richardson, D. M. What attributes make some plant species more invasive?. *Ecology* **77**, 1655–1661 (1996).
65. Guo, X. et al. Variations in the start, end, and length of extreme precipitation period across China. *Int. J. Climatol.* **38**, 2423–2434 (2018).
66. Wang, R., Zhang, J., Guo, E., Zhao, C. & Cao, T. Spatial and temporal variations of precipitation concentration and their relationships with large-scale atmospheric circulations across Northeast China. *Atmos. Res.* **222**, 62–73 (2019).
67. Wan, W. & Zhou, Y. Spatiotemporal patterns in persistent precipitation extremes of the Chinese mainland (1961–2022) and association with the dynamic factors. *Atmos. Res*. 107600 (2024).
68. Dyderski, M. K., Paź, S., Frelich, L. E. & Jagodziński, A. M. How much does climate change threaten European forest tree species distributions?. *Global Change Biol.* **24**, 1150–1163 (2018).
69. Storkey, J., Stratonovitch, P., Chapman, D. S., Vidotto, F. & Semenov, M. A. A process-based approach to predicting the effect of climate change on the distribution of an invasive allergenic plant in Europe. *PloS one* **9**, e88156 (2014).
70. Kurpis, J., Serrato-Cruz, M. A. & Arroyo, T. P. F. Modeling the effects of climate change on the distribution of Tagetes lucida Cav. (Asteraceae). *Global Ecol. Conserv.* **20**, e00747 (2019).

71. Angulo, M. B., do Via Pico, G. & Dematteis, M. Impact of climate change on the current and future distribution of threatened species of the genus Lessingianthus (Vernonieae: Asteraceae) from the Brazilian Cerrado. *Anais da Academia Brasileira de Ciências* **93**, e20190796 (2021).

Acknowledgements
We would like to thank Editage (www.editage.cn) for English language editing.

Author contributions
J.Y. drafted the manuscript, conducted data analysis, and created the figures and tables. L.L. and H.N.Y. conceived the study and revised the manuscript. W.H.Z. and M.Z.H. provided guidance and supervision. J.T.Y. provided the R scripts for the analysis. J.Y., M.Y. and Z.Q.Y. collected and organized the data required for the manuscript.

Funding
This work was supported by the National Natural Science Foundation of China (Grant No. 42461017), Ministry of Science and Technology of the People's Republic of China (Grant No. 2019FY101703), Jilin Province Science and Technology Development Plan (Grant No. YDZJ202201ZYTS478), Jilin Province Science and Technology Development Plan (Grant No. YDZJ202501ZYTS551).

Declarations

Competing interests
The authors declare no competing interests.

Additional information
Supplementary Information The online version contains supplementary material available at https://doi.org/10.1038/s41598-025-93034-0.

Correspondence and requests for materials should be addressed to L.L.